Water Supply

Water Supply Vol 22 No 1, 1075 doi: 10.2166/ws.2021.215

The impact of cables on local scouring of bridge piers using experimental study and ANN, ANFIS algorithms

Rasoul Daneshfaraz[a], Masoud Abam[b], Manouchehr Heidarpour[c], Salim Abbasi[d,*], Mehran Seifollahi[e] and John Abraham[f]
[a] Department of Civil Engineering, Faculty of Engineering, University of Maragheh, Maragheh, Iran
[b] Department of Civil Engineering, Faculty of Engineering, Islamic Azad University of Estahban Branch, Fars, Iran
[c] Department of Water Engineering, Isfahan University of Technology, Isfahan, Iran
[d] Department of Civil Engineering, University of Mohaghegh Ardabili, Ardabil, Iran
[e] Department of Civil Engineering, Faculty of Engineering, University of Tabriz, Tabriz, Iran
[f] School of Engineering, University of St. Thomas, St Paul, MN, USA
*Corresponding author. E-mail: salimabbasi@student.uma.ac.ir

RD, 0000-0003-1012-8342

ABSTRACT

The main purpose of this study was to analyze and predict scour depth and hydraulic performance of piers using soft computing methods and to estimate scour depths using artificial neural networks and ANFIS methods. In the present study, three situations were studied: a rectangular pier without a cable (type I), a rectangular pier with a cable that has a diameter equal to 10% of the pier diameter, and a cable twist angle of 15 degrees (type II), and a rectangular pier with a cable 15% of the pier diameter and an angle of twist of 12 degrees (type III). Tests were carried out with different flow-approach angles: zero, 5, 10, and 15 degrees. Dimensional analysis based on the π Buckingham method was performed. Then, the effect of different parameters, and their importance for estimating scour depth was investigated. Piers with an angle of 15 degrees with respect to the direction of flow had the greatest depth of scouring. Cables can reduce scour depths at this angle; for the second and third classes of piers, the scouring is 10 and 22% compared to the first pier classification. For the second type of pier, angles of 5, 10, and 15 degrees led to increases in scouring depths of 3, 21, and 37% compared to the zero-angle situation.

Key words: bridge pier, cable torsion, collision angle, local scouring, sensitivity analysis

HIGHLIGHTS

- Previous studies have not examined the rectangular bridge piers using cables and measuring the amount of scouring.
- In the present study, the hydraulic performance of bridge piers with cable application as well as estimating scour depth by intelligent ANN and ANFIS methods have been investigated.
- In this study, due to experimental limitations, the ANN and ANFIS methods for higher collision angle flow have also been used.

INTRODUCTION

A major cause of bridge failure is the lack of attention paid to hydraulic standards in their design, implementation, and maintenance. To improve our understanding of bridge failure, a hydraulic study of piers reinforced with cables was performed with a focus on the scouring depths that can occur. There are various ways scouring around piers can be reduced. The use of slots, riprap, collars, submerged plates, and modern methods such as cables and nano clays have been studied for their ability to reduce scouring of sediments (Rezaie *et al.* 2018).

These issues have been studied in prior research. For example, Kumar *et al.* (1999), Osroush *et al.* (2019), and Saleh *et al.* (2020) studied the performance of a slot with changes to its shape and size, the arrangement and placement height of the slot, and piers with different shapes. Chiew (1995), Lauchlan & Melville (2001), Zarrati *et al.* (2010), and Froehlich (2013) investigated the stability of riprap around pier foundations and the temporal changes in geometric and hydraulic parameters. They protected the area around the pier from scouring and reduced scouring.

Zevenbergen *et al.* (2006), Lagasse *et al.* (2010), and Pagliara & Palermo (2020) evaluated scouring from a bridge pier with submerged plates at different establishment levels. In addition to examining scour reduction, they proposed relationships for estimating scour depth. Dey *et al.* (2006) studied flow splitter plates with cables at different torsion angles and different diameters. The study encompassed three bridge piers with different torsion angles and different cable diameters. The experiments showed that the scour depth was reduced by more than 43%. Pandey *et al.* (2018) studied scouring and flow patterns around a circular pier by measuring the components of the meantime velocity using a Doppler velocimeter. The main purpose of this study was to show scour changes by examining the velocity parameters radially and vertically by changing the pier diameter in the flow field. More recently, Majedi-Asl *et al.* (2021) investigated flow with bed grading and sand extraction from the riverbed around a bridge pier group. In total, they performed 22 experiments with two different substrate grades A and B, three different flow discharge rates, and different values of the Froude number. Their results showed that for a Froude number of 0.5, the presence of a pit hole downstream of the pier group causes an increase of 3 and 9.7%, respectively. Izadinia & Heidarpoor (2012a) studied cables and collars on cylindrical piers with differences in diameter and angles of cable twist. The ratio of cable diameter to pier diameter was 0.15 and the torsion angle was 15 degrees. For this situation, the upstream scour depth pier decreased to about 53%. Scouring time was more delayed with the combined use of the cable and collar compared to the collar-only situation. Ghaderi *et al.* (2020) studied the effect of downstream scouring parameters of stepped spillways by changing the flow rates and step sizes. The results of this study showed that the flow regime plays an important role in the dimensions of the scour cavity, also the scour in the side walls is more than the middle of the cross-section. Finally, a relationship was proposed to predict the maximum scour depth. Pandey *et al.* (2020a, 2020b) studied temporal changes in scour depth at the pier of collar-protected circles. The efficiency of the collar, for different diameters and different heights, was investigated in an experimental flume under clear water scouring conditions. The results showed that proper collar performance reduces the maximum scouring depth, and the collar improves the collar performance significantly when installed on the bed surface. Singh *et al.* (2019) investigated the initial scouring of gravel particles cohesionless to mixtures of silt and sand. The results of this study provided an experimental relationship to determine the critical shear stress of sand particles. Daneshfaraz *et al.* (2021a, 2021b) studied the hydraulic performance of a horizontal screen with a variable diameter on a vertical drop in the experimental. The results showed that with increasing the relative diameter of the horizontal screen, the turbulence length increased and the pool depth decreased. Ghaderi *et al.* (2019) studied scouring around the foundations of Simineh Rood Bridge in Miandoab (Iran) using HEC-RAS numerical simulation. Finally, the obtained results were compared with the results and equations of the experimental model. Ghaderi & Abbasi (2019) studied the local scouring of the airfoil-shaped piers with or without collars in the 3D simulation of flow with FLOW-3D software. The results showed that increasing the length of the airfoil reduced the maximum scour depth. The use of a collar on the pier of the airfoil pier reduces the maximum depth of the scouring hole. Pourshahbaz *et al.* (2020) studied the hydro-morphology of the parallel groynes group as a numerical simulation with FLOW-3D software. They also compared the FLOW-3D simulation results with the results of SSIIM 2.0 software. From the results, it was observed that the accuracy of the FLOW-3D simulator was affected by the landing number and the critical speed ratio (U_{avg}/U_{cr}). Singh *et al.* (2020) investigated the scouring of rectangular bridge abutment with clear water. They presented two equations to calculate the maximum scour depth in equilibrium mode and time-dependent scour depth.

Advances in data processing have also impacted hydraulic studies. As an example, data mining is a process that is performed to explore data; the main purpose of data mining is predicting future performance. Multiple data mining methods can be employed. Artificial neural networks (ANN) are made up of simple operating elements that work in parallel. Artificial neural networks can determine the relationships between the inputs and outputs of a system. Adaptive Neuro-Fuzzy Inference Systems (ANFIS) are a combination of neural networks and fuzzy systems based on fuzzy mathematics. This technique has good capabilities for training, construction, and classification.

Ismail (2018) investigated scouring around bridge piers using an evolutionary neural network. The results showed that the model produced estimates of scour equilibrium depth with many fewer constants compared to the hidden layer of neural networks. Sreedhara *et al.* (2019) investigated the prediction of scour depths near a pier bridge by a swarming group of bees based on a neural network and found that for clear water conditions, the PSO-ANN model method outperforms the ANN model. Azamathulla (2012) examined gene expression programming to estimate scour depth downstream of sills. The results showed that the equation proposed by the GEP method compared to other models, to predict the depth of scouring of the sills with different slopes of the bed performed suitably. Pandey *et al.* (2020a, 2020b) Using experimental data, previous researchers examined the maximum scouring depth using genetic algorithms and multiple linear regression. The relationship between

maximum scour depth and the GA method showed more accurate results than MLR. El-Hady Rady *et al.* (2020) predicted the scour depth around a bridge pier using artificial intelligence that was based on conventional regression modeling. Their results showed that the gene programming model is superior to the neuro-fuzzy inference system model. Norouzi *et al.* (2019) used multilayer perceptron (MLP) networks, radial basis function networks, and support vector machines with different kernel functions to estimate the discharge coefficient labyrinth weirs. The results showed that the MLP model had a much higher accuracy than other models. Daneshfaraz *et al.* (2021a, 2021b) investigated the hydraulic performance of vertical drop using a support vector machine, therefore they analyzed hydraulic parameters from 120 different experimental data and 12 support vector machine models.

In previous studies, the phenomenon of scouring near bridge piers has been studied, however the effects of cable supports have not been considered. In addition, while the prediction of scour depth has been investigated previously, the present investigation goes further. Here we wrap the cable around the pier and change the collision angle of the flow to alter the intensity of the downward flow. Other objectives of the research include the following: 1. Investigating the effect of changing the diameter and torsion angle of the cable. 2. The effect of changing the collision angle of the flow to protect the pier and to reduce the scouring depth and also to increase the time required for maximum scouring depth. 3. The use of ANN algorithms and ANFIS to estimate scour depths and then the subsequent comparison of the performance of an artificial neural network with ANFIS. 4. A comparison of the results of the ANNs and ANFIS with experimental results.

MATERIALS AND METHODS

Dimensional analysis

The effective parameters governing scour depth around a bridge pier outfitted with a cable and at a different angle of impact are as follows:

$$\mathrm{F}_1(B, L, P, V, V_c, D_{50}, d_s, t, t_e, g, y, \rho, \rho_s, \upsilon, \alpha, \theta) = 0 \tag{1}$$

The symbol B is the pier width, L refers to pier length, P denotes the cable diameter, V is the flow velocity, V_c represents velocity threshold conditions, D_{50} is the media diameter size, d_s is the final scour depth, t refers to the scour start time, t_e is the scour equilibrium time, g is gravitational acceleration, y refers to the flow depth, ρ is water density, ρ_s is the sediment particle density, υ is kinematic viscosity, α is the flow collision angle, and θ is the angle of twist of the cable. Using Buckingham's theory of dimensional analysis, Equation (1) can be written in dimensionless format as:

$$F_2\left(\frac{gy}{V^2}, \frac{\upsilon}{\rho VD}, \frac{\rho_s}{\rho}, \frac{V}{V_c}, \frac{t}{t_e}, \frac{L}{B}, \frac{P}{B}, \frac{d_s}{B}, \frac{d_{50}}{B}, \frac{y}{B}, P, \alpha, \theta\right) = 0 \tag{2}$$

Due to the constant values of the parameters gy/V^2, ρ_s/ρ, V/V_c, L/B, d_{50}/B, and y/B, and the turbulence of the flow from the above parameters and the Reynolds number $\upsilon/\rho VD$, certain simplifications are possible. By simplifying and combining dimensionless parameters, Equation (2) can be rewritten as:

$$F_3\left(\frac{d_s}{B}, \frac{t}{t_e}, \frac{P}{B}, \alpha, \theta\right) = 0 \tag{3}$$

In the above relation, d_s/B is the final dimensionless scour depth, t/t_e dimensionless scouring time, P/B is the dimensionless cable diameter, α refers to the collision angle, and θ is the cable torsion angle.

Experimental methodologies

The experiments were performed in a rectangular experimental flume with a total length of 14 m, a useful length of 10 m, a width of 0.4 m, and a depth of 0.6 m with a fixed horizontal floor without a slope. The floor of the flume was made of PVC and the walls were made of Plexiglas with a thickness of 10 mm. There is an adjustable gate downstream of the test site that is able to control the water depth in the channel. A constant flow rate of 23 liters per second was regulated by a calibrated valve next to the pump. The range of the experimental portion of the flume is 2 meters long and 0.2 meters wide. To measure the scouring depth, a depth gauge was used. The gauge was movable in all three directions. Table 1 shows the criteria used in the present study.

Table 1 | Criteria for various research studies

Research	Criteria used	Allowed amount	The amount of research present	Reason for review
Raudkivi & Ettema (1983)	The ratio of channel width to pier width (W/B)	6.25	7.65	Due to the lack of effect of the channel walls
Melville & Sutherland (1988)	The ratio of pier width to average grains diameter (b/d_{50})	Larger than 25 to 25	42.85	Due to the elimination of the effect of sediment grains size on scouring depth
Melville & Sutherland (1988)	The geometric standard deviation of sediment grains ($\sigma = d_{84.1}/d_{15.9}$)	Less than 1.3	1.23	Preventing the non-uniformity of sediment grains reduces the depth of scouring equilibrium
Chiew (1995), Ettema (1980) and Shen *et al.* (1969)	Flow depth (y)	More than 4 times the pier diameter	21	To prevent the increase of scouring depth in shallow flows by increase the flow depth
Raudkivi & Ettema (1983)	The average diameter of grains (d_{50})	Greater than or equal to 0.7 mm	0.7 mm	To prevent the formation of ripple phenomenon in non-sticky sediments
Raudkivi & Ettema (1983)	Flow velocity (Vc)	0.9Vc	0.9Vc	To start local scouring in clearwater

Sand with a relative density of 2.65 was used to create the sediment. To ensure the uniformity of sediments, these materials have been passed through two consecutive sieves with 0.59 mm and 0.85 mm pore sizes. Residual sediments between the two sieves were selected for this experiment. These sediments were larger than 0.59 mm and smaller than 0.85 mm in diameter. In the present study, the sediments have $d_{50} = 0.7$ mm and $\sigma = 1.23$.

Raudkivi & Ettema (1983) found timewise changes in scour depth over three consecutive hours to be not more than one millimeter. In the present study, more than 90% of scouring depth occurs in the first 8 hours, so each experiment was limited to an 8-hour duration.

Physical models and experiments

Rectangular piers made of Teflon were used in the experimental fabrication. The width and length of the rectangular pier were 30 and 90 mm, respectively. The experiments were performed according to Figure 1, and the piers were divided into three groups according to Table 2.

Intelligent modeling

Artificial neural network

An ANN is a very simple approach that was developed to model the biological structures found in the human brain (Kim *et al.* 2001; Pourtaghi & Lotfollahi-Yaghin 2013).

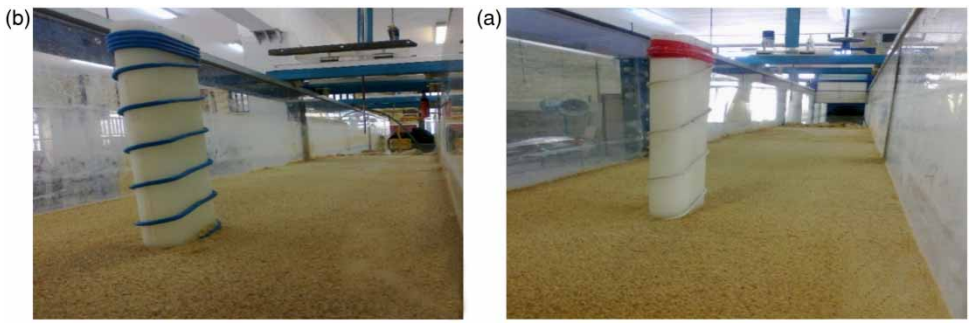

Figure 1 | Rectangular corner round pier. (a) The second type, with a cable 10% of the pier diameter and a cable twist angle of 15 degrees. (b) Third type pier, with 15% cable pier a diameter and cable twist angle of 12 degrees.

Table 2 | Specifications of the present study

Tested piers	Piers diameter (cm)	Cable diameter	Twist angle of the cable (degree)	Collision angle (degree)
P_1	3	Non-cable	Non-cable	0-5-10-15
P_2	3	%10	15	0-5-10-15
P_3	3	%15	12	0-5-10-15

ANN has a multilayered structure that includes many of the key elements of interconnected processing to mimic brain neurons. The neural network contains computational elements called neurons that combine inputs and determine their weight. Because ANN stores data as a template in a set of processing elements adapted from connection weights, complex maps can be identified through distributed representation features (Kim *et al.* 2001). Figure 2 is a representation of the ANN architecture.

In the forward step, the weighted value of the input components is calculated as follows:

$$net_j = \sum_{i=1}^{n} w_{ij} x_{ij} + bias_j \tag{4}$$

where net_j is the weighted sum of the j^{th} neuron for the input received from the preceding layer with n neurons, w_{ij} is the weight between the j^{th} neuron and the i^{th} neuron in the preceding layer; x_i is the output of the i^{th} neuron in the preceding layer. The output of the j^{th} neuron (out_j) is calculated using a sigmoid function as follows:

$$out_j = f(net_j) = \frac{1}{1 + e^{-(net_j)}} \tag{5}$$

This type of layered ANN has been utilized to solve many complex problems (Kartam *et al.* 1997). Details of the learning algorithm can be found in Karayiannis & Venetsanopoulos (2013) and interested readers are directed there.

The adaptive neuro-fuzzy inference system

The compatible ANFIS system consists of 5-layer networks and node connectors. Reasonably structured neuro-fuzzy systems are proportional to input data, membership, rules, and membership functions output. Figure 3 is a representation of neural-fuzzy network architecture with two inputs, one output, and two laws (Aghdam *et al.* 2017).

Determine the structure of the proposed models

For the Levenberh–Margaret neural network algorithm, the number of hidden layers, and the number of neurons in each layer is determined by trial and error. Typically, 8 to 12 neurons are selected. To validate the created neural network, 70%

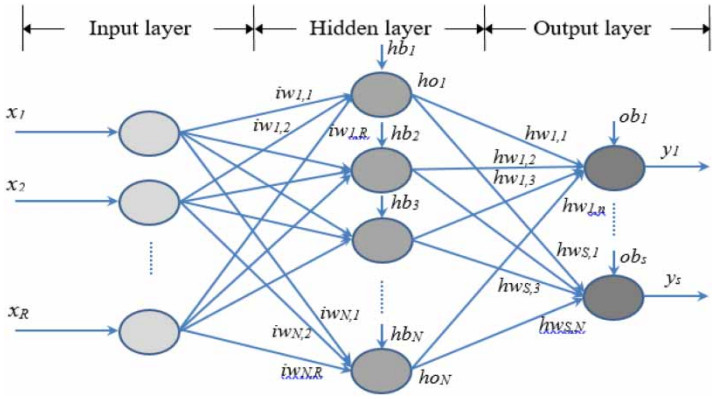

Figure 2 | ANN schematic structure (Choi & Cheong 2006).

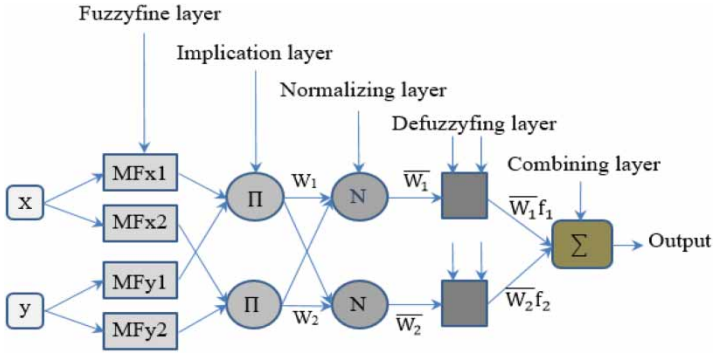

Figure 3 | ANFIS schematic structure (Akib *et al.* 2014).

of the data were selected for training, and the remaining 30% were maintained for validation. The output of the sigmoid excitation function used in the reverse diffusion algorithm is in the range between zero and one, Therefore, the output should be in the same range. Mapping was done using the following general rule:

$$x_n = 0.05 + 0.95\left(\frac{x_i - x_{min}}{x_{max} - x_{min}}\right) \tag{6}$$

The values x_{max}, and x_{min} are the maximum and minimum values in the x_i range, respectively. Network training and network repetition rates of 0.1 and 400 are used, respectively. As the mean square error (MSE) increases, the network training process automatically stops. An ANFIS model to study two membership functions with 100 reps for a variety of membership function is intended. Considering the effect of the membership function and the use of trial and error, the psigmf membership function provided the best results.

Evaluation criteria

To evaluate the performance accuracy of the proposed intelligent models, statistical parameters measuring the correlation between observed and computed values were identified. The selected metrics are: root mean square error (RMSE), mean absolute error (MAE), correlation coefficient (CC), and demonstration coefficient (DC). The relationships of these indices are given in Equations (7)–(10).

$$RMSE = \sqrt{\frac{\sum_{k=1}^{N}(t_k - y_k)^2}{N}} \tag{7}$$

$$C.C = \frac{\sum_{i=1}^{N}(t_{k_i} - \overline{t_k})(y_{k_i} - \overline{y_k})}{\sqrt{\sum_{i=1}^{N}(t_k - \overline{t_{k_i}})^2 \sum_{i=1}^{N}(y_{k_i} - \overline{y_k})^2}} \tag{8}$$

$$D.C = 1 - \frac{\sum_{k=1}^{N}(t_k - y_k)^2}{\sum_{k=1}^{N}(t_k - \overline{t_k})^2} \tag{9}$$

$$MAE = \frac{1}{N}\sum_{i=1}^{N}|y_k - t_k| \tag{10}$$

t_k and y_k are the observed results (experiments) and the output of the neural network, respectively. First, the data were normalized using a Gaussian normalization technique. In the present study, the data were normalized using Equation (6), where x_{min}, x_{max}, respectively, refer to the minimum and maximum data and x_n is the normalized data.

RESULTS AND DISCUSSION

Temporal development of scour depth and the flow collision angle

To investigate the ability of cables to reduce the final scour depth, scour depths in the presence and absence of cables were determined and compared. The final depth was obtained at the end of each experiment. In general, for the second class of piers, the final scour depth is 9.09% less than the first type pier. For the third type of pier, the final scour depth is 10.59 and 18.72% less than the second and first pier types.

Temporal development of scour depth for the first pier and the influence of angle

The temporal development of scour depth for the first pier type and angles of zero, 5, 10, and 15 degrees are provided in Figure 4. Over time, the appearance of horseshoe vortices has also dropped dramatically. These vortices, which enhanced vertical water motions, are primarily responsible for moving and transporting particles. For the first type of pier, a comparison of the 10- and 15-degree cases reveals very small differences, particularly for the first 90 minutes. After 90 minutes, the 15-degree case has a greater slope than the other curves. Also, as the collision angle increases, the scouring depth will increase.

Increasing the collision angle of the flow makes the pier wider and ultimately increases the strength of the horseshoe vortex and increases scouring. For experiments on the first type of pier and at angles of 5, 10, and 15 degrees increases the scouring depth by 4, 20, and 35%, respectively compared to the zero-degree case.

Temporal development of scour depth for the second pier type and the influence of flow angle

In Figure 5, as the angle varies from zero to 5°, there is not much effect on the scour depth. The two scour depth curves coincide from the initial moment until equilibrium. Conversely, for the 10- and 15-degree angles, the scouring experiences equal slopes for 90 minutes. Thereafter, 15 degree pier has a steeper slope. Approximately 3 hours after the start of scouring, they become parallel again. The second type of pier, with an angle of 5 degrees experiences a 12% depth reduction, compared to the first type. The second type pier at an angle of 10 degrees leads to a 10% reduction in final scour depth; a collision angle flow of 15 degrees has the greatest scouring depth. The effect of cables for reducing the scour depth for this angle and for the second type pier is 10%.

For angles of 5, 10, and 15 degrees and for the second class of pier, there is an increase in horseshoe vortex activity and a consequent depth increase of 3, 21, and 37%, respectively (compared to the 0-degree case).

Temporal development of scour depth for the third type of pier and the influence of flow angle

Figure 6 shows photographs of the experimental facility and Figure 7 shows the temporal development of scouring. As seen in the figure, for the first and second pier types, the scouring depths at angles of 10 and 15 degrees and for $d_s/b = 0.2$ differ. The piers with angles of zero and 5 degrees are also almost identical.

For the third pier type, it is observed that at an angle of 5 degrees, the scouring depth is reduced 18% compared to the first pier type. At an angle of 10 degrees, the third class of pier has a 17% reduction in the final scour depth compared to the first pier class. All experiments at the angle of 15 degrees have the most scouring and the effect of cables for reducing scour depth

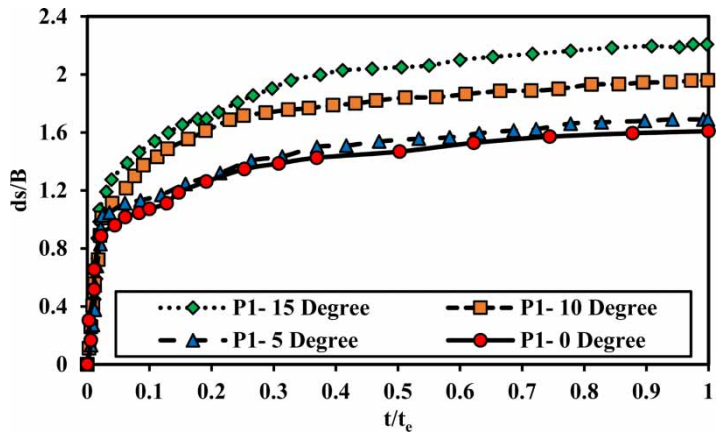

Figure 4 | Temporal development of the first type scour under zero, 5, 10, and 15-degree angles with the flow direction.

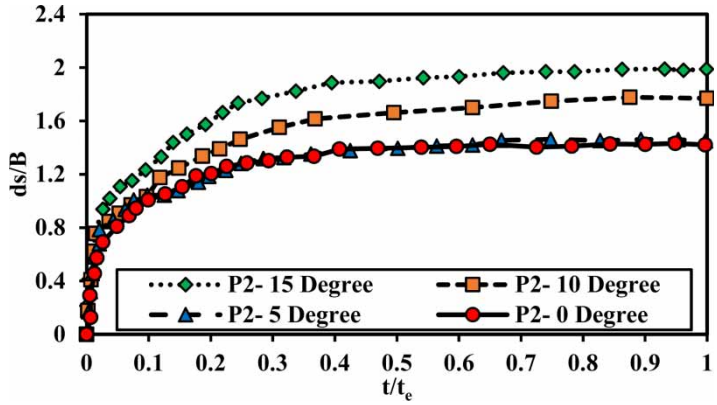

Figure 5 | Temporal development of the second type scour under zero, 5, 10, and 15-degree angles with the flow direction.

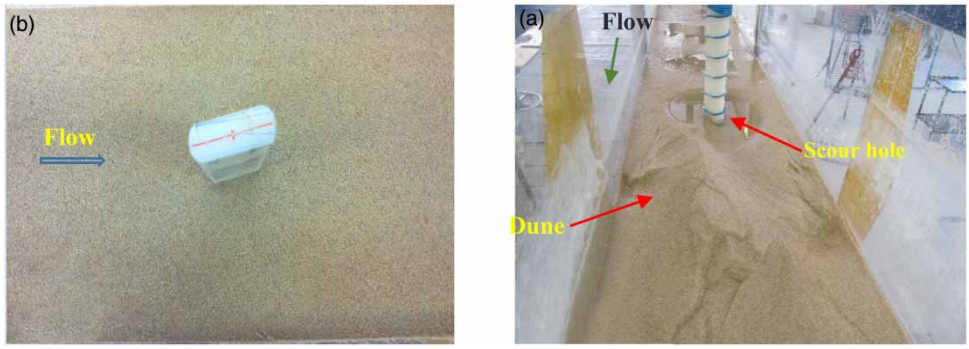

Figure 6 | Scouring at the pier of the third type. (a) Final depth of the scouring of the third type at the collision angle 15 degrees in the downstream position. (b) How to apply the angle change.

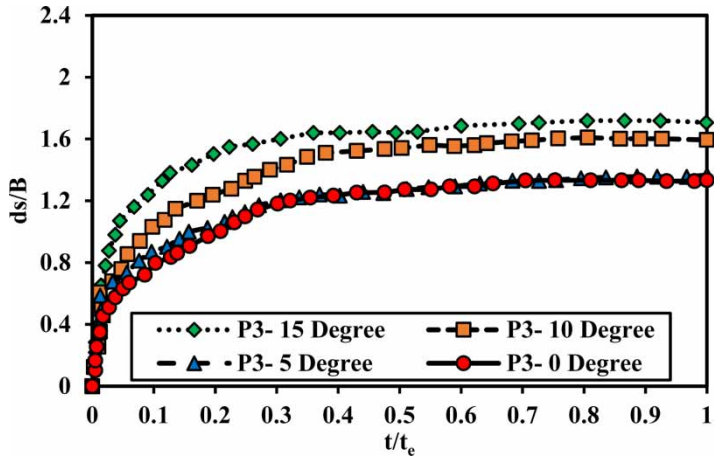

Figure 7 | Temporal development of the third type scour under zero, 5, 10, and 15-degree angles with the flow direction.

(15-degree angle and the third pier type) is 22%. Table 3 shows the reduction of the scour depth for the second and third pier types, compared to the first type of the pier. By comparing Figures 4, 5 and 7, it is concluded that increasing the cable the diameter will reduce the initial scouring depth and the maximum depth.

For the third type of pier, a cable with a diameter 15% that of the pier diameter is used and the cable has a smaller torsion angle, with angles of 5, 10, and 15 degrees compared to the pier, there is a depth increase of 3, 20, and 27%, compared to the

Table 3 | Percentage reduction of the final scour depth compared to the first type of pier for different flow angles (degrees)

Tested piers	Flow collision angle 0 degree	Flow collision angle 5 degree	Flow collision angle 10 degree	Flow collision angle 15 degree
P_2	12	12	10	10
P_3	17	18	17	22

zero-angle case. Consequently, the third pier type with a collision angle of 15 degrees has a lesser scour depth than the first and second pier types. It can be seen that the third pier leads to less total scouring. As evident in Figures 4, 5 and 7 the scour depth for the third pier with a zero-degree angle is reduced by ds/b = 1.3, 1.4, and 1.6, respectively. Such decreases can be seen from other angles as well. The final scour depth for the third pier is 17% less than for the first pier.

Temporal development of scour depth according to the type of pier

Temporal development of scour depth for first, second, and third pier types at zero degrees

Typically, increasing the collision angle of the flow makes the pier wider and increases the power of the horseshoe vortices. Consequently, as the collision angle increases, the depth of scouring also increases. For the second pier type, a thin cable was used. For the first 90 minutes of scouring, the results are similar to the first pier without a cable. The initial scour depth for the third pier is less than the scour for the second pier. Furthermore, the second pier experiences less scouring than the first pier. This finding demonstrates the influence of a cable in reducing scour depth.

Temporal development of scour depth for all three piers at a 5 degree angle

For the three pier types, it was observed that with a flow collision angle of 5 degrees, the scour depth is increased marginally, by 4, 3, and 3%, respectively (compared to the zero-angle situation). As can be seen from Figure 9, when scouring initiates at the third pier, the scour depth is much less than that for the first pier. Therefore, it can be concluded that increasing the diameter of the cable has a significant effect on reducing the depth of scour in the early moments. A comparison of these curves in Figure 9 shows the depth of scouring at this angle for the first type of pier. It is much more than for piers equipped with a cable. The third pier initially prevented the scoured hole from deepening. The final scour depth is closer to the second and third types of piers and is most different compared to the first pier. For all three piers, and for at $t/te = 0.2$, about 90% of the scour depth has developed. Thereafter, the scouring process continues slowly. The results were obtained with a collision angle of the flow of zero and 5 degrees (Figures 8 and 9). The dimensionless depth (ds/B) for the first to third type piers has increased from 1.34, 1.45, and 1.6 to 1.47, 1.5, and 1.67, respectively.

Temporal development of scour depths for all pier types, at a 10-degree angle

For piers with a 10-degree collision angle, the first, second, and third piers experience a scouring depth increase of 20, 21, and 20% respectively, compared to the zero-degree case. This issue can be seen in Figure 10, when compared to Figures 8 and 9.

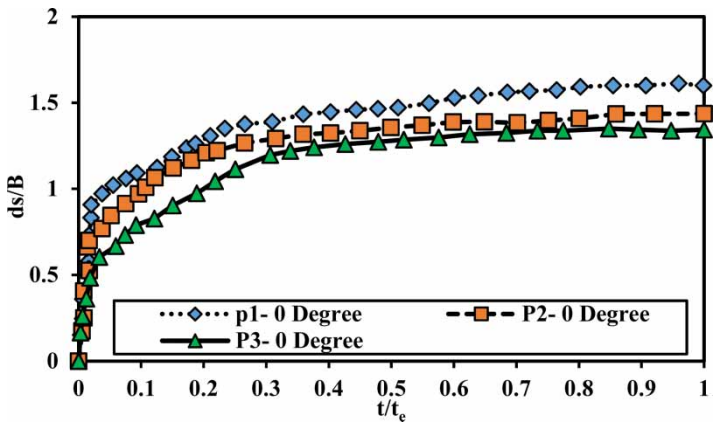

Figure 8 | Temporal development of scour depth for first, second, and third type piers at a zero-degree angle with the flow direction.

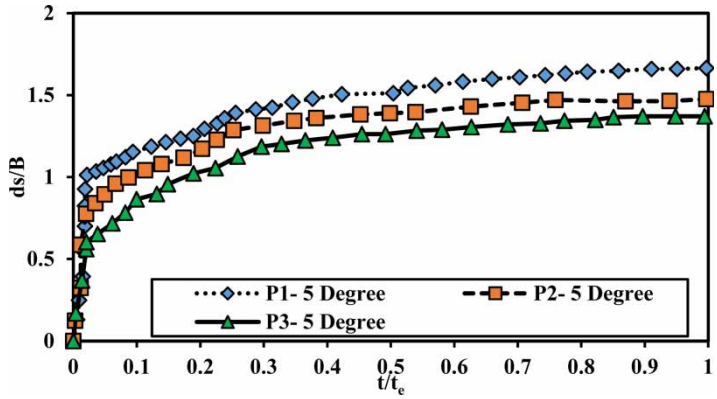

Figure 9 | Temporal development of scour depth for first, second, and third type piers at a 5-degree angle with the flow direction.

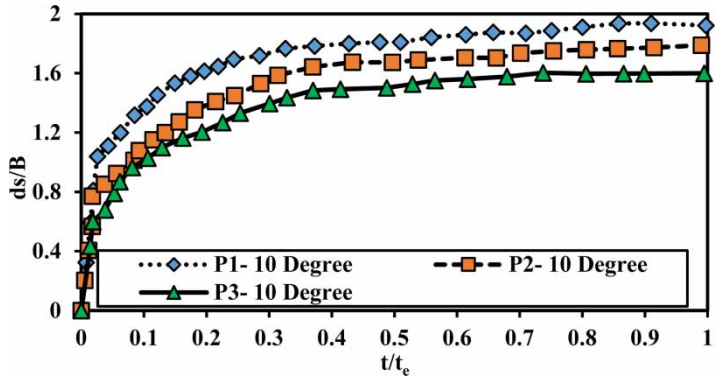

Figure 10 | Temporal development of scour depth for first, second, and third type piers at a 10-degree angle with the flow direction.

The second and third pier curves are similar until $t/t_e = 0.1$. Thereafter, the first pier experiences more scouring than other piers.

Increasing the collision angle of the flow increases the width of the pier and intensifies the downward flow and horseshoe vortices, as already discussed. This leads to an enhancement of vertical flow caused by horseshoe vortices.

Temporal development of scour depths for all three piers, at a 15 degree angle

For all three piers, a cable with a diameter that is 15% of the pier diameter was employed. The cable has a low torsion angle. There are depth increases of 35%, 37%, and 27.5%, respectively, for the three piers, compared to the zero-flow collision angle situation. The diagram in Figure 11 for the second and third pier types shows that the scour depth for piers one and two are very similar, until $t/t_e = 0.2$. A slight difference is observed for the second pier and is probably due to the insufficiency of the thin cable (with a diameter of 10% compared to the pier). Table 4 shows the increase of the final scour depth with collision angles relative to the zero-degree angle case.

To compare the present study with the experimental studies of previous researches, similar models in the same (laboratory) flow conditions should be used. Therefore, similar studies using cables, collars and gaps were used to compare with the present study. For this purpose, the best results of the present study and previous researches have been used in Table 5.

Prediction of scour depth by ANN and ANFIS methods

To predict the scour depth using ANN methods and ANFIS, the 11 models with input parameters listed in Tables 6 and 8 were used. From the 11 models. The optimal structure was determined based on performance criteria for both the learning and testing processes. Next, a membership function was adjusted using a recursive diffusion algorithm in combination with the recursive least squares method. To reduce the MAE, the number of membership functions is gradually increased by reducing the penetration amplitude of the cluster centers using a trial-and-error method. To compare ANN and ANFIS methods, the RMSE, MAE, correlation coefficient (CC), and coefficient of determination (DC) are utilized (see Tables 6 and 8).

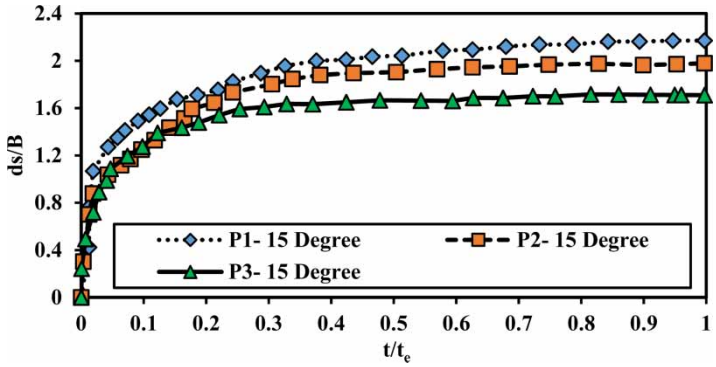

Figure 11 | Temporal development of scour depth for first, second, and third type piers at a 15-degree angle with the flow direction.

Estimations of the final depth of scouring using the ANN method

The 11 models encompass different combinations of input variables to be able to provide the best combination for scouring estimation. The goal is to adjust the models so that the effect of single variables can be analyzed and compared with models that have other input variables. By reviewing the results and considering the evaluation criteria for different models, it was observed that model number 1 is superior compared to the others. This model has the lowest RMSE and MAE (close to zero) and the largest CC and DC (close to one). Table 6 has been prepared to help compare results. It is found that by considering the ratio of cable diameter to pier width (P/B) and comparing scour start time to scour equilibrium time (t/t_e), the effect of the flow collision angle parameter (α) is much more significant than the cable torsion angle parameter (θ). It should be noted that for predictions made with an ANN, models 2 and 4 differ from model 1 by less than 3% in the CC criterion. In other words, the cable diameter parameter to pier width (P/B) has very little effect on scouring.

The diagram in Figure 15 is obtained using the values in Table 6. Values of the performance criteria CC and RMSE are shown as a percentage; values of CC ~ 1 and RMSE ~ 0 signify better performance. According to Table 6, and as mentioned in Figure 12, it can be seen that model number 1 (the superior model) is the best, and model number 2 is next in performance

Table 4 | Percentage increase of scour depth for the case of angled piers relative to a pier with zero degrees angle

Tested piers	Flow collision angle 5 degree	Flow collision angle 10 degree	Flow collision angle 15 degree
P_1	4	20	35
P_2	3	21	37
P_3	3	20	27.5

Table 5 | Comparison of the results of the present study with previous research in similar experimental conditions

Researcher	Research specifications	Pier mechanism	Maximum scour reduction (%)
Dey *et al.* (2006)	Cylindrical single pier	Cable	51.1
Izadinia & Heidarpoor (2012a)	Cylindrical single pier	Cable and Collar	52.18
Aghli and Zomorodian (2014)	Cylindrical bridge pier in meandering river	Cable and Collar	69
Izadinia & Heidarpoor (2012b)	Cylindrical single pier	Cable and Slot	25
Heidarpour *et al.* (2010)	Bridge Pier Groups	Collar	45
Davodi *et al.* (2019)	Bridge Pier Groups	Cable	56
Solimani-Babarsad *et al.* (2021)	Cylindrical single pier	Cable	63
Present study	Triangular bridge pier	Cable	37

Table 6 | Defined models and prediction using the ANN method

			Train				Test			
Row	Models	Max. neuron	CC	DC	MAE	RMSE	CC	DC	MAE	RMSE
1	α, θ, t/t_e, P/B	14	0.9821	0.9644	0.0354	0.0767	0.9843	0.9687	0.0355	0.0750
2	α, θ, t/t_e	12	0.9730	0.9466	0.0540	0.0965	0.9725	0.9457	0.0514	0.0882
3	α, θ, P/B	10	0.7473	0.5578	0.1872	0.2718	0.7448	0.5546	0.1872	0.2775
4	α, t/t_e, P/B	14	0.9731	0.9469	0.0501	0.0939	0.9726	0.9450	0.0520	0.0989
5	θ, t/t_e, P/B	6	0.5741	0.3288	0.2690	0.3363	0.5778	0.3337	0.2698	0.3338
6	α, θ	10	0.7517	0.5648	0.1826	0.2724	0.7254	0.5228	0.1812	0.2754
7	α, t/t_e	14	0.7982	0.6366	0.1716	0.2476	0.7928	0.6284	0.1676	0.2483
8	α, P/B	12	0.7546	0.5692	0.1864	0.2718	0.7135	0.5033	0.1781	0.2776
9	θ, t/t_e	10	0.5689	0.3233	0.2719	0.3395	0.6085	0.3667	0.2566	0.3179
10	θ, P/B	8	0.3562	0.1263	0.3048	0.3873	0.3740	0.1375	0.2823	0.3644
11	t/t_e, P/B	12	0.5773	0.3332	0.2692	0.3359	0.5624	0.3131	0.2686	0.3355

quality. Therefore, these two models have the best accuracy. In addition, model 10 has minimal accuracy according to Table 6 and Figure 12, These observations show that the P/B and θ are unimportant for estimating the final scour depth.

According to the performance criteria studied by the researchers in Table 7, RMSE and R^2 criteria are the most used compared to other criteria. By comparing RMSE and R^2 criteria in the study of Bateni *et al.* (2007) with 98% accuracy, Ismail *et al.* (2013) estimated the scour depth around the bridge pier with 83% accuracy. The present study with RMSE and MAE of 0.075 and 0.035, respectively, has good accuracy. Many studies have been done to estimate scour depth, which is of particular importance to designers because of the importance of scour depth around the bridge pier.

Results of final scour depth estimation by ANFIS method

In this study, 11 models were performed (see Table 8) to estimate the scouring depth with ANFIS. The results and evaluation criteria for different models showed that model 2 is superior. This model has the lowest RMSE and MAE (close to zero) and the highest CC and DC (close to one) compared to other models. According to the results of Table 8, and by comparing models 7 and 9 and also models 8 and 10 with constant values of parameters (t/t_e) and (P/B), the effect of the flow angle parameter (α) is found to be much more significant than the cable torsion angle parameter (θ).

The diagram in Figure 13, corresponds to the values in Table 8. The values of CC and RMSE are shown in the figure as a percentage. The greater the distance between the two lines indicates an improved performance. According to Table 8 and seen in Figure 13, model 2 (a superior model) has the lines with the greatest distance and the maximum accuracy. Model 10 has the lowest distance and minimum accuracy according to Table 8 and Figure 13.

According to Tables 6 and 8, the input parameters are the same in the methods used and in the proposed models. Therefore, the comparison of two methods with the same parameters in the input data has been made. Figure 14, shows a comparison of the top models of the neural network and ANFIS method, As can be seen, the ANN method (see Table 6 and Figure 14) (first

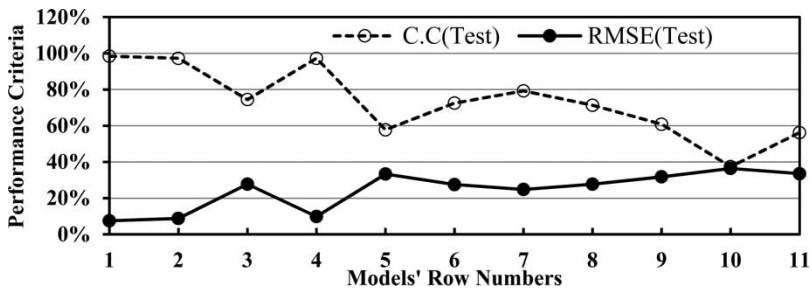

Figure 12 | Diagram of performance criteria of CC. and RMSE for the results predicted by the ANN.

Table 7 | Comparison of the results of the present study with the results of previous researchers in the ANN model

Researcher	Previous research used	CC	MAPE	RMSE	R^2	MAE
Choi & Cheong (2006)	Laursen and Toch (1956)	–	179.15	–	–	–
	Neill (1973)	–	272.33	–	–	–
	Jain and Fischer (1979)	–	436.65	–	–	–
	CSU (Richardson and Davis, 1995)	–	165.39	–	–	–
	Melville (1997)	–	264.98	–	–	–
Lee *et al.* (2007)	Laursen and Toch (1956)	0.8160	–	1.0138	–	–
	Shen (1971)	0.7119	–	0.5994	–	–
	Hancu (1971)	0.7303	–	1.1360	–	–
	Coleman (1971)	0.6786	–	0.4765	–	–
	Ettema *et al.* (1999)	0.7523	–	1.5825	–	–
	BPN (Lee *et al.* 2007)	0.9559	–	0.1393	–	–
Bateni *et al.* (2007)	Laursen and Toch (1956)	–	–	0.0727	0.5288	0.0497
	Shen (1971)	–	–	0.0640	0.5815	0.0444
	Hancu (1971)	–	–	0.1188	0.3284	0.0720
	Breusers *et al.* (1977)	–	–	0.1039	0.1221	0.0613
	Melville & Sutherland (1988)	–	–	0.1326	0.5350	0.0761
	Melville (1997)	–	–	0.0589	0.6000	0.0411
	Melville and Chiew (1999)	–	–	0.0519	0.6074	0.0393
	ANN (MLP/BP) (Bateni *et al.* 2007)	–	–	0.0078	0.9879	0.0051
	ANN (RBF/OLS) (Bateni *et al.* 2007)	–	–	0.0251	0.8422	0.0180
Ismail *et al.* (2013)	Melville and Chiew (1999)	–	–	0.21914	0.6020	–
	Laursen and Toch (1956)	–	–	0.21295	0.5195	–
	Shen (1971)	–	–	0.20828	0.4604	–
	HEC-18, US DoT (1995)	–	–	0.20065	0.5943	–
	GRNN (Ismail *et al.* 2013)	–	–	0.13876	0.7240	–
	Sigmoid network (Ismail *et al.* 2013)	–	–	0.10570	0.8366	–
	Optimised network (Ismail *et al.* 2013)	–	–	0.09301	0.8725	–
Zounemat-Kermani & Teshnehlab (2008)	Salim and Jones (1996)	–	–	1.497	0.366	1.12
	HEC-18 (2001)	–	–	1.064	0.726	0.77
	Sheppard and Glasser (2004)	–	–	0.991	0.818	0.697
	Ataie-Ashtiani and Beheshti (2006)	–	–	0.821	0.866	0.649
	FFBP-NN (Zounemat-Kermani & Teshnehlab 2008)	–	–	0.39	0.966	0.27
	RBF-NN (Zounemat-Kermani & Teshnehlab 2008)	–	–	0.53	0.936	0.37
Present study		0.9843	–	0.075	–	0.035

Table 8 | Defined models and predictions using the ANFIS method

		Train				Test			
Row	models	CC	DC	MAE	RMSE	CC	D.C	MAE	RMSE
1	α, θ, t/t_e, P/B	0.9626	0.9265	0.0489	0.1009	0.7260	0.3076	0.2792	0.3082
2	α, θ, t/t_e	0.9626	0.9265	0.0489	0.1009	0.7626	0.3258	0.1760	0.2213
3	α, θ, P/B	0.7712	0.5947	0.1610	0.2370	0.5307	0.5846	0.3069	0.3393
4	α, t/t_e, P/B	0.9626	0.9265	0.0489	0.1009	0.7145	0.0248	0.2220	0.2662
5	θ, t/t_e, P/B	0.6773	0.4587	0.2135	0.2738	0.0302	2.3428	0.4357	0.4928
6	α, θ	0.7712	0.5947	0.1610	0.2370	0.5312	0.1001	0.2098	0.2557
7	α, t/t_e	0.8090	0.6545	0.1529	0.2188	0.5222	0.2193	0.2132	0.2976
8	α, P/B	0.7712	0.5947	0.1610	0.2370	0.5309	0.2056	0.2596	0.2960
9	θ, t/t_e	0.6773	0.4587	0.2135	0.2738	0.0302	2.3428	0.4357	0.4928
10	θ, P/B	0.4862	0.2364	0.2520	0.3253	0.0000	1.8596	0.4180	0.4558
11	t/t_e, P/B	0.6773	0.4587	0.2135	0.2738	0.0302	2.3428	0.4357	0.4928

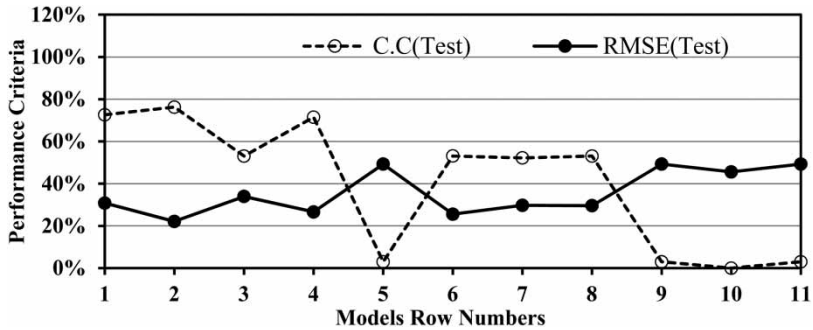

Figure 13 | Curve of CC and RMSE performance criteria for the results predicted by ANFIS.

model CC = 0.9843) has better accuracy than the ANFIS method (second model CC = 0.7626). While the ANFIS method is generally not able to predict scour depths that are in good agreement with experimental results. The numbers provide an underestimate to the final scour depth. If it is necessary to use the proposed methods in practice, it is enough to present the maximum amount of error obtained from the method to the proposed value.

The Table 9 is the results of validation data for researchers who used ANFIS to predict scour depth. Due to the large effect of the number of data and input variables on the inference and according to the fuzzy system computational algorithm, the results of this method, like the neural network method, are in an acceptable range, but it still has less adaptation than the neural network. Due to the fact that in this study only nine different experimental models have been investigated in different conditions, there is not suitable scope for adaptation to the ANFIS computational algorithm. For this reason, it has shown poorer performance in estimation, which can be remedied by performing more and various experiments.

Sensitivity analysis

To evaluate the effect of input variables on the output predictions, the neural network sensitivity analysis (superior method) was used. With this method, the inputs to a statistical model are changed in a systematic way so that the effects of these changes can be identified:

$$Effectiveness(\%) = \left|\frac{CC\ (ALL\ Var) - CC\ (Var_i)}{CC\ (ALL\ Var)}\right| \times 100 \tag{11}$$

By removing each parameter from the series of input parameters, the impact of the parameters could be assessed. The effect of parameter removal on the accuracy of the overall model was quantified using the statistical parameters RMSE, MAE, CC, and DC.

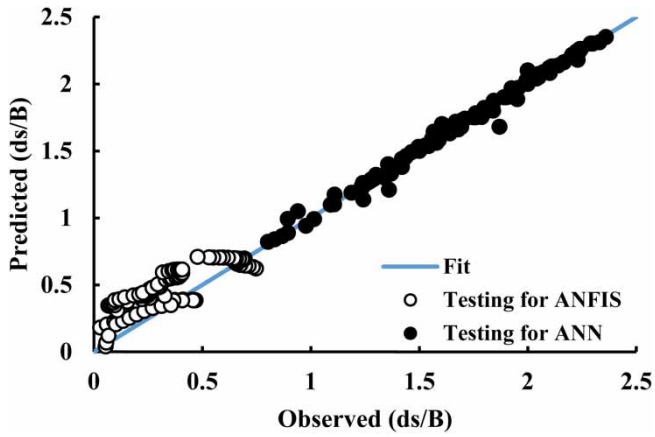

Figure 14 | Comparison of superior models of methods ANN and ANFIS.

Table 9 | Comparison of the results of the present study with the results of previous researchers in the ANFIS model

Researcher	MAPE	RMSE	R	MAE
Azamathulla (2012)	–	0.290	0.960	–
Najafzadeh *et al.* (2013)	0.726	0.530	0.960	–
Moradi *et al.* (2018)	7.87	0.154	0.970	–
Muzzammil and Alam (2011)	4.160	0.050	0.950	–
Azimi *et al.* (2019)	–	0.135	0.978	–
Azamathulla & Ghani (2011)	–	0.0046	0.941	1.426
Najafzadeh *et al.* (2016)	27.54	0.0281	0.89	–
Present study	–	0.221	0.762	0.1760

As can be seen from the results of the sensitivity analysis in Table 10, by removing the α parameter, the accuracy of the results was drastically reduced. The α parameter has the largest effect among the input parameters. the effect of this parameter compared to the total input parameters is a 40.31% reduction in accuracy. Data corresponding to Table 10 are shown in Figures 15 and 16. Also, the L/B parameter according to Table 10 has less sensitivity in estimating the final scour depth.

CONCLUSION

In this study, the performance and efficiency of cable in controlling local scour around the pier of a rectangular bridge by changing the flow collision angle were investigated and presented in experimental and intelligent algorithms. Based on the results, by increasing the cable diameter, the initial and final scouring depth can be reduced. The reason for this is to reduce the downward flow and weaken the horseshoe vortices. Using different experimental models, the scouring method and the final scouring depth reduction by cable are described. The general results are as follows:

Table 10 | The relative impact of each of the input parameters in the superior model

	Train				Test				
Variable	CC	DC	MAE	RMSE	CC	DC	MAE	RMSE	Effectiveness (%)
α	0.57	0.33	0.27	0.34	0.59	0.34	0.26	0.34	40.31
θ	0.97	0.93	0.05	0.10	0.97	0.94	0.05	0.11	1.28
t/t_e	0.74	0.55	0.18	0.27	0.76	0.57	0.19	0.28	22.80
P/B	0.97	0.95	0.05	0.09	0.98	0.96	0.05	0.09	0.24
L/B	0.98	0.97	0.04	0.07	0.98	0.97	0.04	0.07	0.15
V/V_C	0.98	0.96	0.04	0.09	0.98	0.97	0.04	0.07	0.33
All Vars	0.98	0.95	0.04	0.09	0.98	0.96	0.04	0.08	–

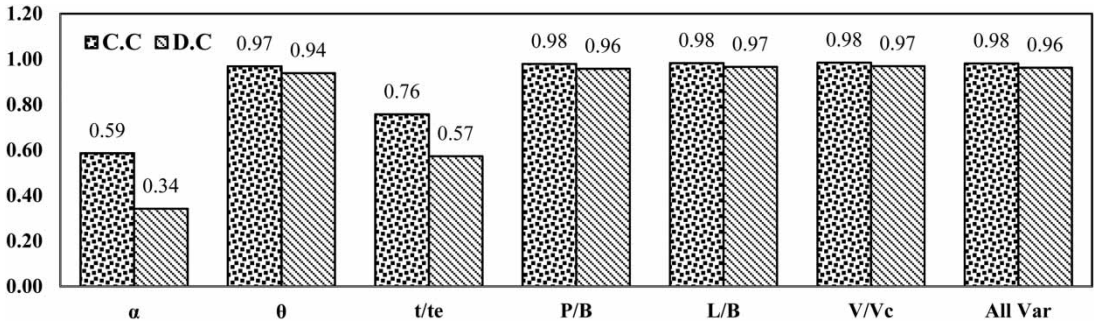

Figure 15 | Values of performance criteria by deleting the desired parameter.

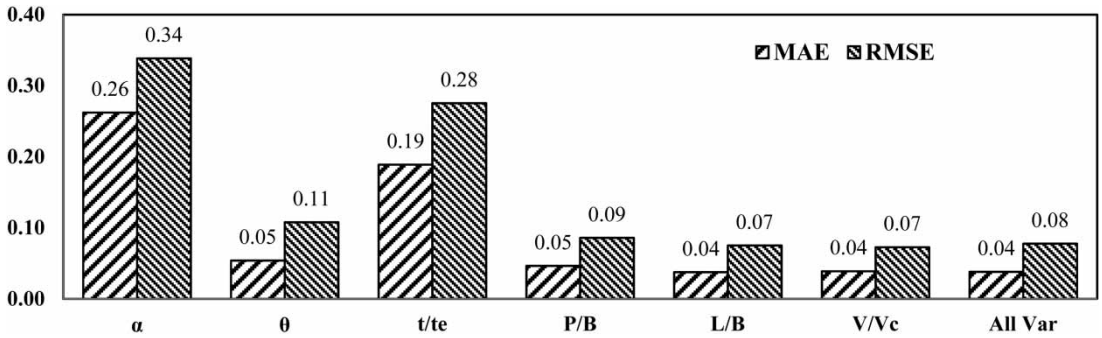

Figure 16 | Values of performance criteria by deleting the desired parameter.

1. Wrapping the cable around the bridge pier (with diameters of 10 and 15% of the pier diameter) and angles of 15 ° and 12 ° will reduce the depth of the scour pit by up to 22%.
2. For the first, second, and third foundation types, scouring starts upstream of the bridge pier and after about 3 hours, it extends downstream of the pier at the nose.
3. At the beginning of scouring, the presence of horseshoe vortices on both sides of the pier deposit sediments downstream of the pier. After three hours, it reaches the initial depth and is washed.
4. For the second and third pier types, the rate of scouring is somewhat slower compared to the first pier type.
5. Reducing the angle of twist of the cable around the pier reduces the depth of scouring. If the cable twists are close together, the number of turns of available cables increases and this reduces the scouring depth.
6. By increasing the flow collision angle to the pier of the bridge, the scour depth increases. Changing the angle by more than 10 degrees is not recommended.
7. Analysis using ANN and ANFIS methods showed a high capability for estimating scour depth. It was also observed that the model with input parameters α, θ, t/t_e, P/B and using a neural network method has the highest accuracy and efficiency with the highest correlation coefficient and coefficient of explanation (CC and DC) and the lowest error (RMSE).
8. The results of the sensitivity analysis showed that by removing the input parameter α, the model error rate increases to a large extent (40.31%). Therefore, this parameter is the most important variable for estimating scour depth.

DATA AVAILABILITY STATEMENT

All relevant data are included in the paper or its Supplementary Information.

REFERENCES

Aghdam, I. N., Pradhan, B. & Panahi, M. 2017 Landslide susceptibility assessment using a novel hybrid model of statistical bivariate methods (FR and WOE) and adaptive neuro-fuzzy inference system (ANFIS) at southern Zagros mountains in Iran. *Journal of Environmental Earth Sciences* **76**, 1–22.

Aghli, M. & Zomorodian, S. 2014 Effect of combination wrapping cable and collar on depth of scour around cylindrical bridge pier groups on rivers meander. *Iranian Journal of Soil and Water Research* **45** (1), 1–10. https://doi.org/10.22059/ijswr.2014.51166.

Akib, S., Mohammadhassani, M. & Jahangirzadeh, A. 2014 Application of ANFIS and LR in prediction of scour depth in bridges. *Journal of Computers & Fluids* **91**, 77–86. https://doi.org/10.1016/j.compfluid.2013.12.004.

Ataie-Ashtiani, B. & Beheshti, A. A. 2006 Experimental investigation of clear-water local scour at pile groups. *Journal of Hydraulic Engineering* **132** (10), 1100–1104.

Azamathulla, H. M. 2012 Gene expression programming for prediction of scour depth downstream of sills. *Journal of Hydrology* **460**, 156–159.

Azamathulla, H. M. & Ghani, A. A. 2011 ANFIS-based approach for predicting the scour depth at culvert outlets, *Journal of Pipeline Systems Engineering and Practice* **2** (1), 35–40.

Azimi, H., Bonakdari, H., Ebtehaj, I., Shabanlou, S., Talesh, S. H. A. & Jamali, A. 2019 A pareto design of evolutionary hybrid optimization of ANFIS model in prediction abutment scour depth. *Sādhanā* **44** (7), 1–14.

Bateni, S. M., Borghei, S. M. & Jeng, D. S. 2007 Neural network and neuro-fuzzy assessments for scour depth around bridge piers. *Engineering Applications of Artificial Intelligence* **20** (3), 401–414.

Breusers, H. N. C., Nicollet, G. & Shen, H. W. 1977 Local scour around cylindrical piers. *Journal of Hydraulic Research* **15** (3), 211–252.

Chiew, Y. M. 1995 Mechanics of riprap failure at bridge piers. *Journal of Hydraulic Engineering* **121**, 635–643. https://doi.org/10.1061/(ASCE)0733-9429(1995)121:9(635).

Choi, S. U. & Cheong, S. 2006 Prediction of local scour around bridge piers using artificial neural networks. *Journal of the American Water Resources Association (JAWRA)* **42**, 487–494. https://doi.org/10.1111/j.1752-1688.2006.tb03852.x.

Coleman, N. L. 1971 Analyzing laboratory measurements of scour at cylindrical piers in sand beds. *Proceeding of the 14th IAHR Congress, Paris, France* **3**, 307–313.

Daneshfaraz, R., Bagherzadeh, M., Esmaeeli, R., Norouzi, R. & Abraham, J. 2021a Study of the performance of support vector machine for predicting vertical drop hydraulic parameters in the presence of dual horizontal screens. *Journal of Water Supply* **21** (1), 217–231.

Daneshfaraz, R., Ghaderi, A., Francesco, S. D. & Khajei, N. 2021b Experimental study of the effect of horizontal screen diameter on hydraulic parameters of vertical drop. *Journal of Water Supply*. https://doi.org/10.2166/ws.2021.077

Davodi, H., Masjedi, A. R., Heidarneja, M., Bordbar, A. & Kamanbedast, A. A. 2019 Investigation of the effect of cable on the control of scour around the piles group in the river. *JWSS* **23** (2), 73–86.

Dey, S., Sumer, B. M. & Fredsce, J. 2006 Control of scour at vertical circular piles under waves and current. *Journal of Hydraulic Engineering* **132**, 279–270. https://doi.org/10.1061/9780784482971.008.

El-Hady Rady, R. A. 2020 Prediction of local scour around bridge piers: artificial-intelligence-based modeling versus conventional regression methods. *Journal of Applied Water Science* **10** (57), 1–11. https://doi.org/10.1007/s13201-020-1140-4.

Ettema, R. 1980 *Scour at Bridge Piers*. Department of Civil Engineering, University of Auckland Rep. No. 216, Auckland, New Zealand.

Ettema, R. E., Melville, B. W. & Barkdoll, B. 1999 Closure. A scale effect in pier-scour experiments[J]. *Journal of Hydraulic Engineering, ASCE* **125** (8), 895–896.

Froehlich, D. C. 2013 Protecting bridge piers with loose rock riprap. *Journal of Applied Water Engineering and Research* **1**, 39–57. https://doi.org/10.1080/23249676.2013.828486.

Ghaderi, A. & Abbasi, S. 2019 CFD simulation of local scouring around airfoil-shaped bridge piers with and without collar. *Sādhanā* **44** (10), 1–12.

Ghaderi, A., Daneshfaraz, R. & Dasineh, M. 2019 Evaluation and prediction of the scour depth of bridge foundations with HEC-RAS numerical model and empirical equations (Case study: bridge of Simineh Rood Miandoab, Iran). *Engineering Journal* **23** (6), 279–295.

Ghaderi, A., Daneshfaraz, R., Torabi, M. A., Abraham, J. & Azamathulla, H. M. 2020 Experimental investigation on effective scouring parameters downstream from stepped spillways. *Journal of Water Supply* **20** (5), 1988–1998.

Hancu, S. 1971 Sur le calcul des affouillements locaux dams la zone des piles des ponts. *Proceedings of the 14th IAHR Congress. Paris, France* **3**, 299–313.

Heidarpour, M., Afzalimehr, H. & Izadinia, E. 2010 Reduction of local scour around bridge pier groups using collars. *International Journal of Sediment Research* **25** (4), 411–422.

Ismail, A. 2018 Prediction of scour depth around bridge piers using evolutionary neural network. *Journal of Mathematical Modelling in Civil Engineering* **14**, 26–36. https://doi.org/10.2478/mmce-2018-0005.

Ismail, A., Jeng, D. S., Zhang, L. L. & Zhang, J. S. 2013 Predictions of bridge scour: application of a feed-forward neural network with an adaptive activation function. *Engineering Applications of Artificial Intelligence* **26**(5–6), 1540–1549.

Izadinia, E. & Heidarpoor, M. 2012a Simultaneous use of cable and collar to prevent local scouring around bridge pier. *International Journal of Sediment Research* **27**, 394–401.

Izadinia, E. & Heidarpoor, M. 2012b Investigation and comparison of efficiency of cable and groove in protection against scouring. *Engineering and Irrigation Sciences (Scientific Journal of Agriculture)* **37** (1), 1–12.

Jain, S. C. & Fischer, E. E. 1979 *Scour around circular bridge piers at high Froude numbers*. No. FHWA-RD-79–104 Final Rpt.

Karayiannis, N. & Venetsanopoulos, A. N. 2013 *Artificial Neural Networks: Learning Algorithms, Performance Evaluation, and Applications*. Springer Science & Business Media, New York, p. 209.

Kartam, N., Flood, I. & Garrett, J. H. 1997 *Artificial Neural Networks for Civil Engineers: Fundamentals and Application*. American Society of Civil Engineers, New York, NY.

Kim, C., Bae, G., Hong, S., Park, C., Moon, H. & Shin, H. 2001 Neural network based prediction of ground surface settlements due to tunnelling. *Journal of Computers and Geotechnics* **28**, 517–547. https://doi.org/10.1016/S0266-352X(01)00011-8.

Kumar, V., Raju, K. G. R. & Vittal, N. 1999 Reduction of local scour around bridge piers using slots and collars. *Journal of Hydraulic Engineering* **125**, 1302–1305. https://doi.org/10.1061/(ASCE)0733-9429(1999)125:12(1302).

Lagasse, P. F., Zevenbergen, L. W. & Clopper, P. E. 2010 Impacts of debris on bridge pier scour, J. of HENRY Hydraulic Engineering Repository. In: *Proceeding 3rd International Conference on Scour and Erosion (ICSE-5)*, November 7–10, Amsterdam, the Netherlands. CURNET, Gouda (NL), pp. 854–863, https://doi.org/10.1061/41147(392)85.

Lauchlan, C. S. & Melville, B. W. 2001 Riprap protection at bridge piers. *Journal of Hydraulic Engineering* **127**, 412–418. https://doi.org/10.1061/(ASCE)0733-9429(2001)127:5(412).

Laursen, E. M. & Toch, A. 1956 Scour around bridge piers and abutments. *Iowa Highway Research Board* **4**, 60.

Lee, T. L., Jeng, D. S., Zhang, G. H. & Hong, J. H. 2007 Neural network modeling for estimation of scour depth around bridge piers. *Journal of Hydrodynamics* **19**, 378–386.

Majedi-Asl, M., Daneshfaraz, R., Abraham, J. & Valizadeh, S. 2021 Effects of hydraulic characteristics, sedimentary 3 parameters, and mining of bed material on scour depth of bridge pier groups. *Journal of Performance of Constructed Facilities* **35** (2), 04020148.

Melville, B. W. 1997 Pier and abutment scour: integrated approach. *Journal of Hydraulic Engineering* **123** (2), 125–136.
Melville, B. W. & Chiew, Y. M. 1999 Time scale for local scour at bridge piers. *Journal of Hydraulic Engineering* **125** (1), 59–65.
Melville, B. & Sutherland, A. 1988 Design method for local scour at bridge piers. *Journal of Hydraulic Engineering* **114**, 1210–1226. https://doi.org/10.1061/(ASCE)0733-9429(1988)114:10(1210).
Moradi, F., Bonakdari, H., Kisi, O., Ebtehaj, I., Shiri, J. & Gharabaghi, B. 2018 Abutment scour depth modeling using neuro-fuzzyembedded techniques. *Marine Georesources and Geotechnology* **37**, 1–11.
Muzzammil, M. & Alam, J. 2011 ANFIS-based approach to scour depth prediction at abutments in armored beds. *Journal of Hydroinformatics* **13** (4), 699–713.
Najafzadeh, M., Barani, G. A. & Hessami-Kermani, M. R. 2013 Abutment scour in clear-water and live-bed onditions by GMDH network. *Water Science and Technology* **67** (5), 1121–1128.
Najafzadeh, M., Etemad-Shahidi, A. & Lim, S. Y. 2016 Scour prediction in long contractions using ANFIS and SVM. *Ocean Engineering* **111**, 128–135.
Neill, C. R. 1973 *Guide to Bridge Hydraulics. Roads and Transportation*. Association of Canada, University of Toronto Press, Toronto, Canada.
Norouzi, R., Daneshfaraz, R. & Ghaderi, A. 2019 Investigation of discharge coefficient of trapezoidal labyrinth weirs using artificial neural networks and support vector machines. *Applied Water Science* **9** (7), 1–10.
Osroush, M., Hosseini, S. A., Kamanbedast, A. A. & Khosrojerdi, A. 2019 The effects of height and vertical position of slot on the reduction of scour hole depth around bridge abutments. *Ain Shams Engineering Journal* **10**, 651–659. https://doi.org/10.1016/j.asej.2019.02.004.
Pagliara, S. & Palermo, M. 2020 Effects of bridge pier location and debris accumulation on equilibrium morphology. *World Environmental and Water Resources Congress* **1**, 76–83.
Pandey, M., Sharma, P. K., Ahmad, Z., Singh, U. K. & Karna, N. 2018 Three-dimensional velocity measurements around bridge piers in gravel bed. *Marine Georesources & Geotechnology* **36** (6), 663–676.
Pandey, M., Zakwan, M., Khan, M. A. & Bhave, S. 2020a Development of scour around a circular pier and its modelling using genetic algorithm. *Water Supply* **20** (8), 3358–3367.
Pandey, M., Azamathulla, H. M., Chaudhuri, S., Pu, J. H. & Pourshahbaz, H. 2020b Reduction of time-dependent scour around piers using collars. *Ocean Engineering* **213**, 107692.
Pourshahbaz, H., Abbasi, S., Pandey, M., Pu, J. H., Taghvaei, P. & Tofangdar, N. 2020 Morphology and hydrodynamics numerical simulation around groynes. *ISH Journal of Hydraulic Engineering* **8**, 1–9.
Pourtaghi, A. & Lotfollahi-Yaghin, M. A. 2013 Hydrodynamic inline force prediction on vertical cylinders: a comparative study of neural network and its adaptive wavelets (Wavenets). *Journal of Marine Science and Technology* **18**, 418–434.
Raudkivi, A. J. & Ettema, R. 1983 Clear-water scour at cylindrical piers. *Journal of Hydraulic Engineering* **109**, 338–350. https://doi.org/10.1061/(ASCE)0733-9429(1983)109:3(338).
Rezaie, M., Daneshfaraz, R. & Dasineh, M. 2018 Experimental investigation of adding clay and PAM on scour reduction bridge piers under the influence removal of river materials. *Journal of Hydraulics* **13** (3), 59–70. doi:10.30482/jhyd.2018.81358.
Richardson, E. V. & Davis, S. R. 1995 Evaluating scour at bridges. In: FHWA-IP-90–017, *Hydraulic Engineering Circular No. 18 (HEC-18) (3rd edn), Office of Technology Applications, HTA-22, Federal Highway Administration*, US Department of Transportation, Washington, DC, USA.
Saleh, H. H., Darweesh, M. S. & Abozeid, G. 2020 Reduction of local scour around oblong bridge piers using slots. *Journal of Advanced Engineering Trends* **39**, 45–62. doi:10.21608/JAET.2020.75171.
Salim, M. & Jones, J. S. 1996 Scour around exposed pile foundations. In *North American Water and Environment Congress & Destructive Water*, 2202–2211, ASCE.
Shen, H. W. 1971 *River Mechanics*. Vol. 2. New York, USA: John Wiley and Sons.
Shen, H. W., Schneider, V. R. & Karaki, S. 1969 Local scour around bridge piers. *Journal of the Hydraulics Division* **95**, 1919–1940.
Sheppard, M.D. & Glasser, T. L. 2004 Sediment scour at piers with complex geometries. In *Proceedings 2nd International Conference on Scour and Erosion (ICSE-2).* November 14.–17, 2004, Singapore.
Singh, U. K., Ahmad, Z., Kumar, A. & Pandey, M. 2019 Incipient motion for gravel particles in cohesionless sediment mixtures. *Iranian Journal of Science and Technology, Transactions of Civil Engineering* **43** (2), 253–262.
Singh, R. K., Pandey, M., Pu, J. H., Pasupuleti, S. & Villuri, V. G. K. 2020 Experimental study of clear-water contraction scour. *Water Supply* **20** (3), 943–952.
Solimani-Babarsad, M., Safaei, A. & Aghamajidi, R. 2021 Laboratory study of cable and sill protection on scouring pattern around the bridge pier. *Iranian Journal of Soil and Water Research* **52** (2), 523–538.
Sreedhara, B. M., Kuntoji, G., Manu, M. & Mandal, S. 2019 Application of particle swarm based neural network to predict scour depth around the bridge pier. *Journal Intelligent Systems and Applications* **11**, 38–47.
US DoT 1995 Recording and coding guide for the structure inventory and appraisal of the nation's bridges, *US Department of Transportation, Bridge Management Branch*.
Zarrati, A. R., Chamani, M. R., Shafaie, A. & Latifi, M. 2010 Scour countermeasures for cylindrical piers using riprap and combination of collar and riprap. *International Journal of Sediment Research* **25**, 313–322. https://doi.org/10.1016/S1001-6279(10)60048-0.

Zevenbergen, L. W., Lagasse, P. F., Clopper, P. E. & Spitz, W. J. 2006 Effects of debris on bridge pier scour. In: Verheij, H. J. & Hoffmans, G. J. *Proceeding 3rd International Conference on Scour and Erosion (ICSE-3)*, November 1–3, Amsterdam, the Netherlands. CURNET, Gouda (NL), pp. 741–749. https://doi.org/10.1061/40927(243)376.

Zounemat-Kermani, M. & Teshnehlab, M. 2008 Using adaptive neuro-fuzzy inference system for hydrological time series prediction. *Applied Soft Computing* **8** (2), 928–936.

First received 18 May 2021; accepted in revised form 22 June 2021. Available online 5 July 2021